Elastomers and Composites
Vol. 58, No. 3 pp. 142~151 (September 2023)

Print ISSN 2092-9676/Online ISSN 2288-7725
DOI: https://doi.org/10.7473/EC.2023.58.3.142

Thermal, Curing, Elastic, and Mechanical Properties of Ethylene Propylene Diene Monomer/Polybutadiene/Carbon Black Composites

Tae-Hee Lee and Keon-Soo Jang†

Department of Polymer Engineering, School of Chemical and Materials Engineering, The University of Suwon, Hwaseong, Gyeonggi-do, 18323, Republic of Korea

(Received Septembert 15, 2023, Revised Septembert 22, 2023, Accepted Septembert 26, 2023)

Abstract: In this study, we investigate the thermal and mechanical properties of composites comprising ethylene propylene diene monomer (EPDM) and polybutadiene (PB) obtained using carbon black (CB) as a reinforcing and compatibilizing filler. Owing to the significance of elastomeric materials in various industrial applications, blending of EPDM and PB has emerged as a strategic method to optimize the material properties for specific applications. This study offers insights into the blend composition, its microstructure, and the resulting macroscopic behaviors, focusing on the synergetic effects of composite materials. Furthermore, this study delves into curing and rheological behaviors, crosslink densities, and mechanical, thermal, and elastic properties of the elastomeric composites. Through systematic exploration, we believe that this study will be beneficial to material scientists and engineers working on developing advanced elastomeric composites.

Keywords: Rubber, elastomer, composite, polybutadiene (PB), ethylene propylene diene monomer (EPDM), carbon black

Introduction

Elastomeric materials, owing to their unique combination of flexibility and resilience, have been widely used in numerous industrial applications, from automotive to construction sectors.[1-4] Among the diverse family of elastomers, ethylene propylene diene monomer (EPDM) and butadiene rubber (PB) stand out due to their specific mechanical and thermal properties. EPDM, characterized by its superior weather resistance, thermal stability, impermeability and dielectric properties, is extensively utilized in automotive weatherstripping, roofing membranes, and as insulating materials in electrical applications.[5,6] Additionally, its inherent resistance to ozone, UV and oxidation ensures prolonged operational life, making it a material of choice for outdoor applications.[7,8] On the other hand, PB, primarily known for its high resilience and abrasion resistance, finds widespread use in tire, plastic composites, golf balls, and electronic devices.[9-11] Its high resilience ensures energy efficiency in dynamic applications, while its abrasion resistance ensures durability.[12]

Blending polymers including rubbers, such as EPDM and PB, is a strategic approach to tailor the material properties for specific end-use applications, thereby achieving a balance of performance characteristics that may be hard to achieve with individual polymers.[13,14] Such blends can potentially exhibit a synergy of properties, allowing for enhancements in areas like thermal resistance, mechanical strength, aging properties, and processability. However, understanding the nature of interactions, morphology, and resulting properties of EPDM/PB blends is essential for optimizing their composition and processing conditions.

This paper delves into the thermal and mechanical properties of EPDM/PB blends, focusing on the relationship between blend composition, microstructure, and macroscopic behavior. Through a systematic investigation, we aim to provide insights that can guide material scientists and engineers in the development of high-performance EPDM/PB blend-based materials suitable for a wide range of applications.

Experimental

1. Materials

Ethylene propylene diene monomer (EPDM; KEP 330, specific gravity : 0.86) was obtained from Kumho Polychem Co. (South Korea), and polybutadiene (PB; KBR-01, specific

†Corresponding author E-mail: ksjang@suwon.ac.kr

gravity : 0.91), also known as butadiene rubber (BR), was purchased from Kumho Petrochemical Co. (South Korea). Carbon black (CB; FEF) with a diameter of 40-48 nm was obtained from TSR Co. (South Korea). Stearic acid (SA), zinc oxide (ZnO), sulfur, tetramethylthiuram disulfide (TMTD), and 2,2-dibenzothiazole disulfide (DM) were acquired from Puyang Willing Chemical Co. (China). Toluene was purchased from BNOChem Co. (South Korea)

2. Rubber Compounding

The mastication, also known as pre-mixing, of EPDM and PB was performed using an open two-roll mill until a unified blend was achieved. Subsequently, 5 parts per hundred rubber (phr) ZnO and 2 phr SA were integrated into the EPDM/PB rubber blend and compounded for 20 min. This resulting blend is typically termed the 'carbon master batch (CMB)'. 1phr TMTD, 0.6 phr DM, and 1.5 phr sulfur were added to the CMB, leading to the formation of the rubber blend. This final product is commonly designated as the 'final master batch (FMB)'. A comprehensive list of recipes for the rubber compounds is presented in Table 1. In this investigation, alphanumeric designations are employed for each sample. For example, the code E10/CB30 denotes a composition of 100 wt% EPDM with 30 phr of CB and E9B1/CB30 corresponds to a composition comprising 90 wt% EPDM, 10 wt% PB, and 30 phr CB. The contents of additives except CB were identical for this study.

3. Characterization

3.1. Curing and Rheological Properties

3.1.1. Rheometer

The rheological properties of the rubber, including the time required for torque to achieve 90% of its maximum during curing (T_{90}), scorch time (Ts2), curing rate index (CRI), and delta torque (ΔM), were assessed at 160°C using a rubber rheometer (DRM-100, Deakyung Engineering Co., South Korea). An average was taken from two measurements for each sample.

3.1.2. Mooney viscosity

The Mooney viscosity of the rubber samples was measured using a Mooney viscometer (DWV-200C, Deakyung Engineering Co., South Korea) at 125°C for 4 min. Each sample was pre-heated at 125°C for 1 min for stabilization prior to the measurement. An average value was calculated from two determinations for each sample.

3.2. Crosslink density

To evaluate the crosslink density, samples (ca. 1 mg) were immersed in toluene for 24 h. The weight of the dried samples was recorded. For each sample, an average crosslink density was calculated from three measurements.

3.3. Mechanical Properties

3.3.1. Tensile Properties

Uniaxial tensile testing followed the ISO 37 protocol, using a universal testing machine (UTM; DUT-500CM, Daekyung Engineering Co., South Korea). The test specimen had a cross-section of 15 mm × 4 mm and a gauge length of 40 mm. The elongation process was set at a crosshead speed of 500 mm/min under a 5 kN load cell at ambient temperature. The average value was calculated using five specimens.

Table 1. Recipes of the Rubber Compounding

	Rubber Matrix (wt%)							
	EPDM	PB	EPDM /CB30	PB /CB30	E9B1 /CB30	E8B2 /CB30	E7B3 /CB30	E6B4 /CB30
PB	-	100	-	100	10	20	30	40
EPDM	100	-	100	-	90	80	70	60
	Additive (phr)							
Zinc oxide	5	5	5	5	5	5	5	5
stearic acid	2	2	2	2	2	2	2	2
CB	-	-	30	30	30	30	30	30
TMTD	1	1	1	1	1	1	1	1
DM	0.6	0.6	0.6	0.6	0.6	0.6	0.6	0.6
Sulfur	1.5	1.5	1.5	1.5	1.5	1.5	1.5	1.5

3.3.2. Hardness

The Shore A hardness of the rubber blends and composites was determined as per ISO 48 using a hardness tester (306L, Pacific Transducer Instruments, Los Angeles, CA, USA). Results were averaged based on five specimens.

3.4. Elastic Properties

3.4.1. Rebound Resilience

The rebound resilience of the samples was measured in accordance with ISO 4662, utilizing a ball rebound tester (H090, UTS International Co., China). Prior to testing, specimens were maintained at room temperature for 24 h. A ball was dropped onto each sample, and the rebound height was measured. For each sample, the mean was calculated from five measurements.

3.4.2. Compression Set

Tests for compression set followed ISO 815 guidelines. The specimens were set in a cylindrical mold, measuring 12.5 mm (±0.5 mm) × 9 mm, and compressed at 125°C for 22 h. After compression, the specimen was extracted and given a 30-minute recovery period. The final dimensions, particularly height, of the specimens were recorded. The average value was determined based on four specimens.

3.5. Morphological Properties

Surface structures of the EPDM, PB, EPDM/PB blends, and EPDM/PB/CB composites were visualized using a scanning electron microscope (SEM; Apro, FEI Co., Hillsboro, OR, USA) at an electron beam voltage of 10.0 kV. Prior to SEM evaluation, the surfaces, which were fractured during tensile tests, were coated for 3 min with a 5-10 nm gold layer using a sputter coater (Cressington 108 Auto Sputter Coater, Ted Pella Inc., Redding, CA, USA).

3.6. Thermal Properties

To measure the degradation point (T_d) of the rubber composite, thermogravimetric analysis (TGA; Perkin Elmer Co, MA, USA) was conducted according to ISO 11358 standards. The sample of the rubber composite was heated at a rate of 10°C/min from 50°C to 600°C and then maintained at 600°C for 10 min prior to cooling. Measurements were carried out under a nitrogen atmosphere with a nitrogen pressure of 2.2 bar and a flow rate of 20.0 mL/min. The T_d was measured based on 30%, 50%, and 70% weight loss.

Results and Discussions

1. Morphological Properties

In the realm of polymer blends and composites, morphology is important as it directly correlates with both mechanical and thermal properties. The interfacial morphology of each pristine rubber and EPDM/PB composites was probed using SEM. Figure 1 delineates the SEM images of the fractured EPDM/PB surface. Distinct morphologies for unaltered EPDM and PB are illustrated in Figures 1a and 1b, respectively. Despite the incorporation of CB, microfissures persist on the surfaces of composites enriched with EPDM (Figure 1c) and PB (Figure 1d). Figures 1e-1h offer a visualization of the morphology variation in CB-infused composites across different EPDM and PB ratios. The E9B1/CB30 composite, with the minimal PB in the EPDM/PB, showed the most uniform surface. A plausible explanation hinges on the prevalence of more vinyl groups within PB's main chain than in EPDM's ethylidene norbornene (ENB) units, enhancing compatibility due to similar vinyl group concentrations between E9 and B1.

2. Curing and Rheological Properties

Rheometer analyses, as seen in Figures 2a-2c, reveal the curing and rheological dynamics of the vulcanized EPDM/PB/CB composites. The incorporation of CB into EPDM and PB observably diminished T_{90} values, attributed to CB serving as an aiding agent in cross-linking.[15] The addition of CB also increased the curing rate index (CRI), which indicates cross-linking rate, as shown in Figure 2b. The curing rate index (CRI) was calculated based on Equation (1):

$$CRI = \frac{100}{(T_{90} - Ts2)} \quad (1)$$

Even though the presence of CB generally leads to a reduction in Ts2, the inherent compatibility of PB with CB subtly increased Ts2, as depicted in Figure 2c. Mooney viscosity tests, a staple for gauging the viscosity of uncured rubber, indicated enhanced processability of EPDM with CB incorporation, as shown in Figure 3. Concurrently, synergy of CB with PB accelerated cross-linking reactions, amplifying the Mooney viscosity, which contributed well to the curing outcomes.

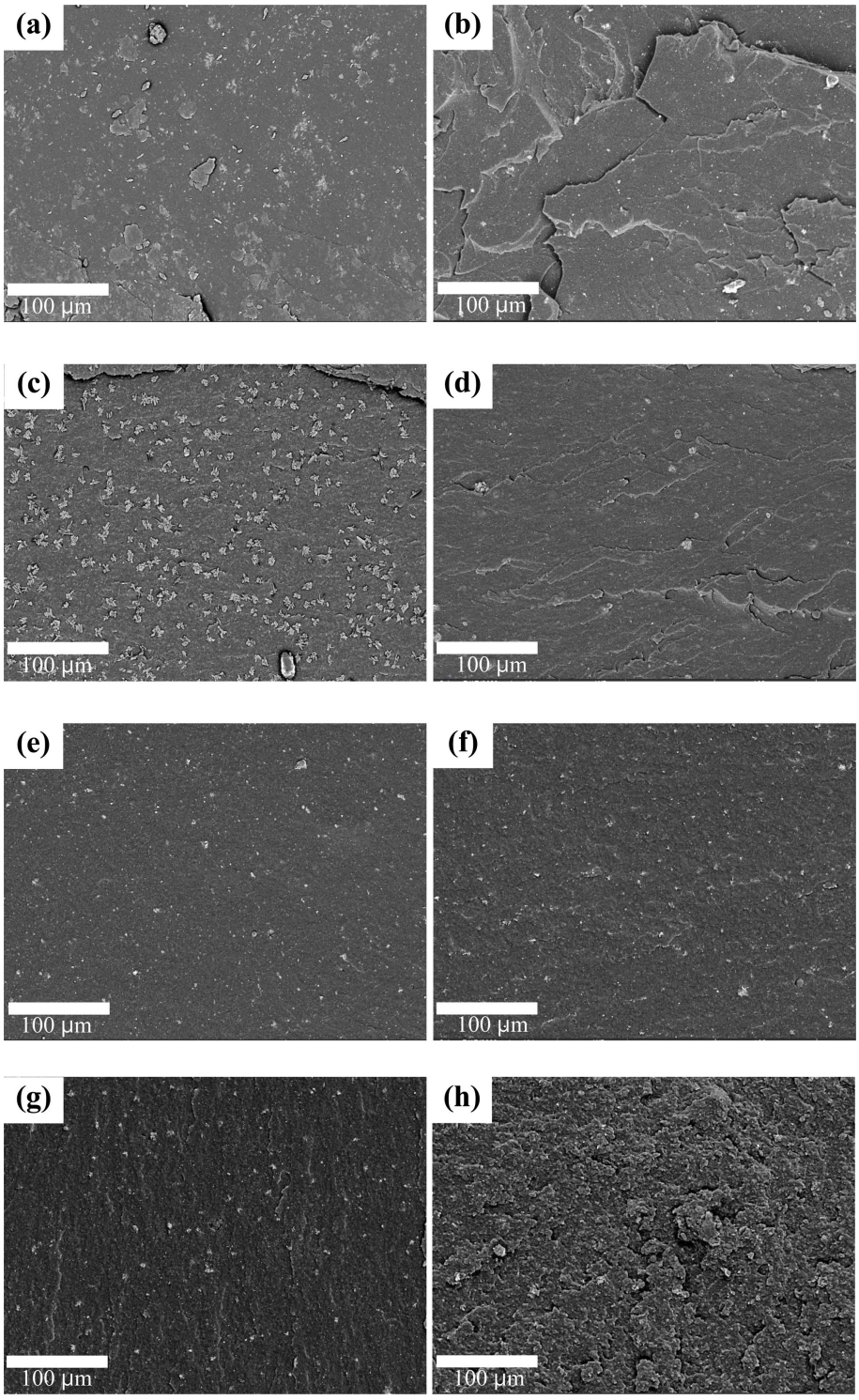

Figure 1. SEM images of fractured surface of rubber and EPDM/PB/CB composites: (a) EPDM, (b) PB, (c) EPDM/CB30, (d) PB/CB30, (e) E9B1/CB30, (f) E8B2/CB30, (g) E7B3/CB30, and (h) E6B4/CB30

3. Crosslink Density

Swelling test data convey a correlation between swelling, ΔM values (Maximum torque – minimum torque during vulcanization), and the crosslink density of rubber composites. ν_e is defined for a perfect network as the number of elastically active network chains per unit volume and is given by:

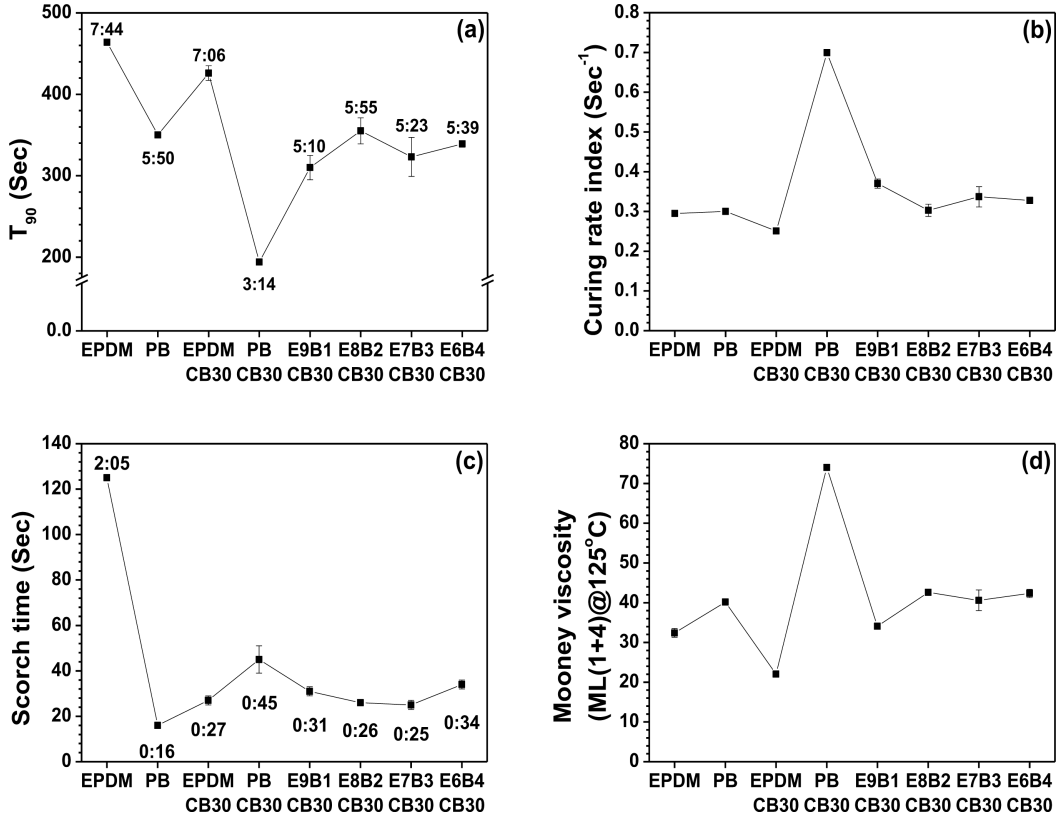

Figure 2. Curing and rheological properties of each rubber and EPDM/PB/CB composites: (a) T_{90}, (b) curing rate index (CRI), (c) scorch time (Ts2), and (d) Mooney viscosity.

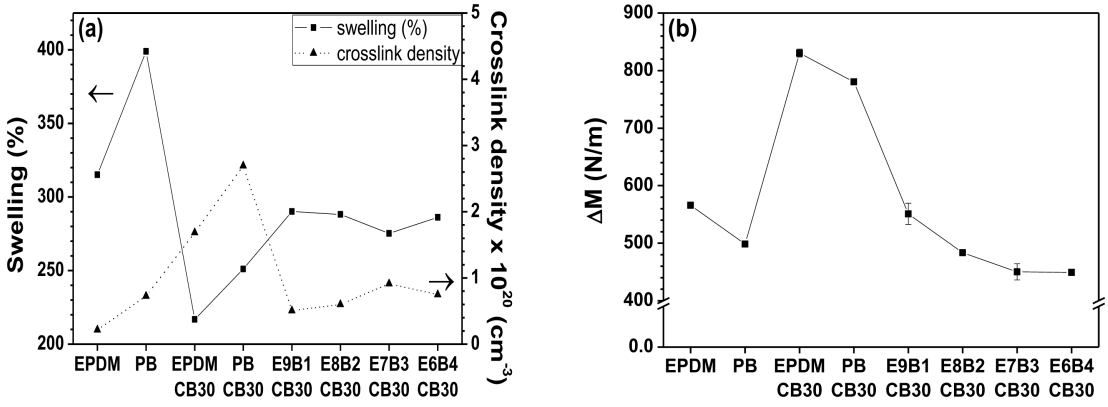

Figure 3. Swelling tests of EPDM/PB/CB composites: (a) swelling index with crosslink-density and (b) ΔM.

$$\nu_e = \rho_p N_A / M_c \quad (2)$$

The average molecular weight of the polymer between cross-links (M_c) according to Flory-Rehner relation:[16]

$$M_c = \rho_p \nu_s \nu_r^{1/3} / -\ln(1-\nu_r) + \nu_r + \chi \nu_r^2 \quad (3)$$

where ν_s is molar volume of the solvent (106.3 cm^3/mol for toluene) and ν_r is the volume fraction of swollen rubber and given by following relation:

$$\nu_r = 1/(1+Q) \quad (4)$$

where Q is defined as a mass of solvent per mass of rubber hydrocarbon and calculated by:

$$Q = (W - W_d)/W_d \quad (5)$$

where W is the weight of the sample soaked in the solvent

for 24 h and W_d is the weight of the sample 30 days after the swelling test.

The ρ_p is a specific gravity of polymer calculated according to the following equation:

$$\rho_p = \frac{W_a}{W_a - W_s} \times \rho_{specific\ gravity\ of\ water} \quad (6)$$

where W_a and W_s are the weight in air and in water, respectively. The χ is the Flory-Huggins interaction parameter, which can be determined by:[17]

$$\chi \cong 0.34 + v_s(\delta_s - \delta_r)^2/RT \quad (7)$$

where δ_s is the solubility parameter of solvent (toluene = 18.3 $(MPa)^{0.5}$) and δ_r is the solubility parameter of polymer [(δ_{EPDM} = 16.6 $(MPa)^{0.5}$), (δ_{PB} = 15.8 $(MPa)^{0.5}$), (e.g. E9B1 = $\delta_{EPDM} \times 0.9 + \delta_{PB} \times 0.1$)].[18,19] $\chi_{(EPDM)}$ = 0.609 and $\chi_{(PB)}$ = 0.4644 were calculated using equation (7). R is the gas constant (8.3144598 J/mol) and T is the testing temperature (room temperature). Low swelling index and high ΔM values indicate high crosslink density of the rubber composites. In Figure 3a, the incorporation of CB into each pristine rubber and

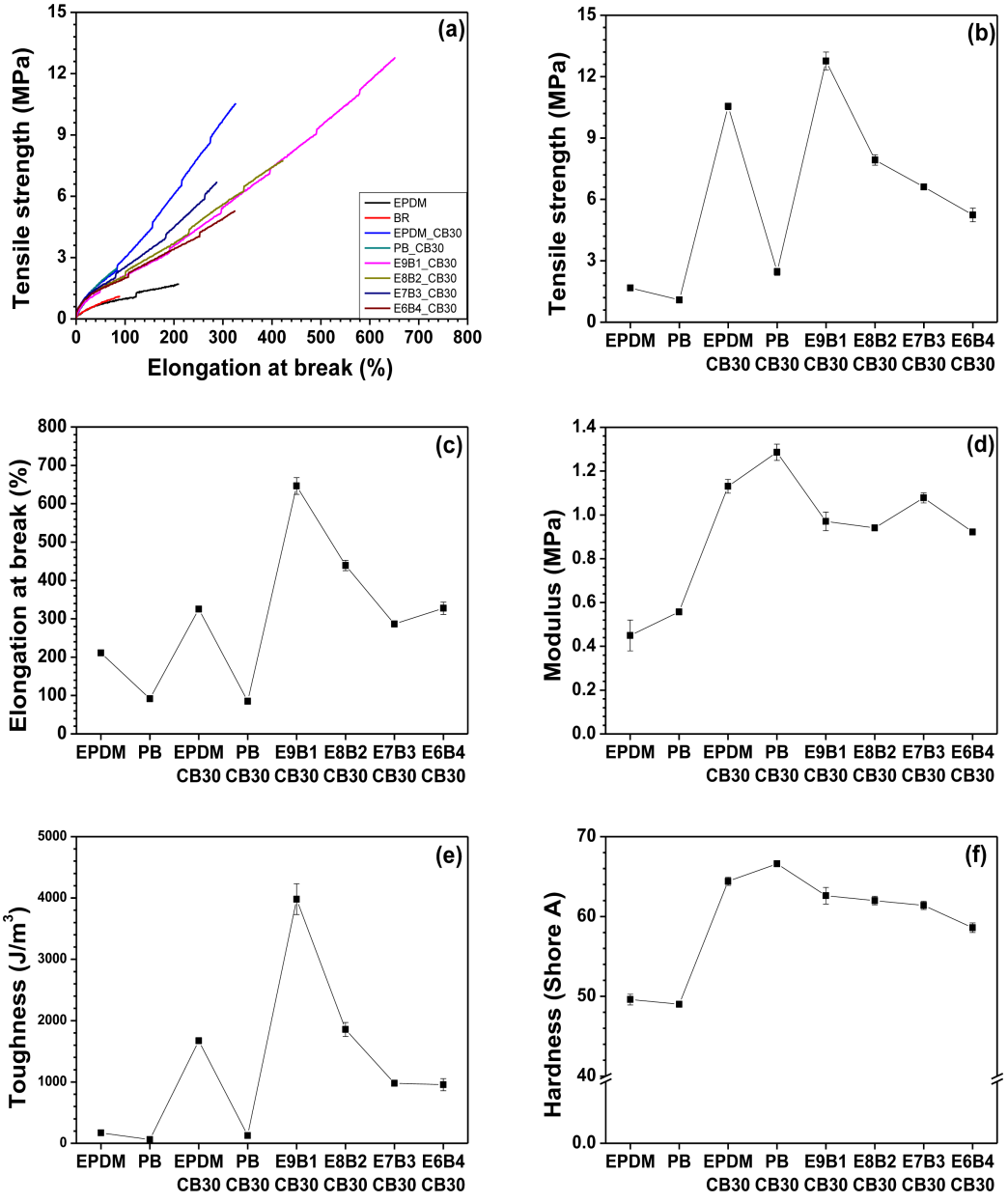

Figure 4. Mechanical properties of EPDM/PB/CB composites: (a) SS-curve, (b) tensile strength, (c) elongation at break, (d) modulus, (e) toughness and (f) hardness.

the EPDM/PB decreased the swelling index. Because CB served as a non-absorbing filler and aided in cross-linking as discussed, the swelling of the composites with added CB was lower than that of EPDM and PB. When examining ΔM, the value for the PB and EPDM with added CB was high (Figure 3b), which suggests that it had the highest crosslink density. This indicates that CB improved the crosslink density of rubber composites. The crosslink densities of EPDM and its associated composites were higher than those of PB and its associated composite. Thus, the crosslink density of EPDM/PB/CB composite increased as a function of PB concentration.

4. Mechanical Properties

Mechanical properties of rubber and composites were examined using UTM.[20-22] The incorporation of CB into either EPDM or PB exhibited an enhancement in tensile strength. The inherent tensile strength of EPDM used in this study was slightly higher than that of PB. The compatibility of CB appeared more harmonious with the EPDM matrix than PB, resulting in higher strength in the former. The strength of EPDM/PB/CB composites decreased with increasing PB content, except for E9B1/CB30, which represented the highest tensile strength. This indicates a heightened compatibility interplay between EPDM and PB in the E9B1/CB30 matrix. The elongation at break for pristine EPDM outperformed that for PB, with E9B1/CB30 emerging as the highest, as shown in Figure 4c. The tendency of toughness was analogous to that of tensile strength. The highest toughness was also achieved for E9B1/CB30 composite among all. The substantial increment for E9B1/CB30 in mechanical properties particularly including toughness indicated that the ratio between EPDM and PB was optimum, exhibiting synergy. The mechanical-morphological property alignment corroborated superior compatibility of E9B1/CB30 and subsequent property elevation. The modulus and hardness of the composites were substantially enhanced by the infiltration of CB, owing to the reinforcing effect of CB.

5. Elastic Properties

The compression set for pristine PB, PB/CB30, and E6B4/CB30 was low because of PB's excellent ability to recover to its original state especially when subjected to heat and pressure (Figure 5a). As discussed in mechanical results, the reinforcing impact of CB in EPDM was substantially higher than that in PB system. Thus, the rebound resilience of EPDM/CB30 was low, as shown in Figure 5b. The rebound resilience of E9B1/CB30 composite was the lowest and that of E6B4/CB30 composite the highest among the EPDM/PB composites. The resilience properties were enhanced by increasing PB concentration. It should be noted that the compression set and rebound resilience values are typically opposite. However, because of distinction in the measuring environment, the values can be parallel. For instance, both compression set and rebound resilience values of a specific elastomer can increase simultaneously.

Both compression set and rebound resilience were evaluated for rubbers and their composites under distinct conditions: heat and pressure for the former, and impact load for the latter. The compression set quantifies the irreversible deformation experienced by elastomers when subjected to defined compression, duration, and temperature. In contrast, rebound resilience measures the proportion of kinetic energy that rubber-like materials recover upon impact. This param-

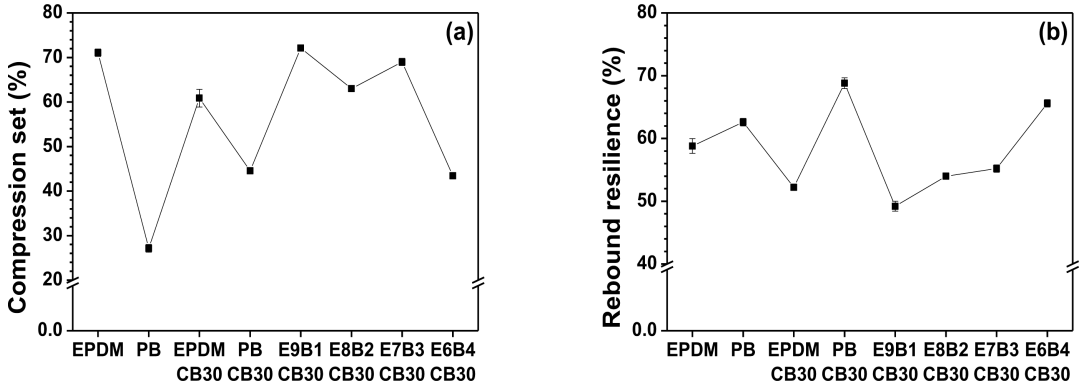

Figure 5. Elastic properties of EPDM/PB/CB composites: (a) Compression set and (b) rebound resilience.

eter is modulated by factors such as the elastomer's type, its specific formulation, and the testing temperature.

The low compression set values observed for pristine PB, PB/CB30, and E6B4/CB30 attest to PB's intrinsic capability to revert to its initial form, particularly under thermal and compressive stresses (Figure 5a). Turning to rebound resilience, Figure 5b highlights that the E6B4/CB30 composite surpasses its counterparts in the EPDM/PB series, exhibiting the maximum elasticity upon impact. The elastic properties were enhanced by increasing PB concentration. It is conventionally believed that compression set and rebound resilience values exhibit inverse trends. However, given variations in testing environments, these metrics can, intriguingly, exhibit concurrent trends. As an illustration, a specific elastomer can exhibit simultaneous increments in both its compression set and rebound resilience.

6. Thermal Properties

To measure the thermal stability, the degradation point (T_d) was evaluated through TGA. TGA quantifies the mass variation in EPDM/PB composites as a direct response to temperature fluctuations, offering insights into the rubber's inherent thermal stability. The exact values of T_d derived from Figure 6 are delineated in Table 2. Compared to EPDM and PB, CB-embedded rubber composites showed a higher T_d. This indicates that CB improved the thermal stability. Especially for E9B1/CB30, the T_d at 70 wt% loss was higher by approximately 70°C relative to other rubber composites in the study. The high compatibility between EPDM and PB contributed more to the enhancement of the thermal stability afforded by CB.

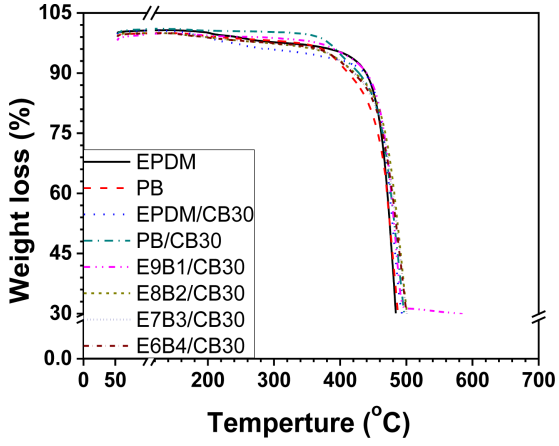

Figure 6. TGA curves of EPDM/PB/CB composites with different blending ratios.

Table 2. Degradation Point (T_d) of EPDM/PB/CB composites

	Thermogravimetric analysis (°C)		
	30 wt% loss	50 wt% loss	70 wt% loss
EPDM	456.8	475.9	484.1
PB	463.2	476.4	487.4
EPDM/CB30	468.6	480.4	493.3
PB/CB30	469.0	483.6	496.8
E9B1/CB30	470.7	482.7	576.7
E8B2/CB30	473.7	488.4	501.3
E7B3/CB30	471.2	487.0	500.9
E6B4/CB30	469.7	486.3	500.4

Conclusion

In this investigation, the thermal and mechanical properties of composites composed of EPDM, PB, and CB were systematically examined. The research underscored the role of blend composition, microstructure, and resulting properties of these elastomeric materials. Morphological examinations, using SEM, revealed surface structures with various ratios, with E9B1/CB30 composite displaying the most uniform surface, likely due to similar vinyl group concentrations. Curing and rheological analyses showed the accelerated cross-linking dynamics and increased curing rate index with the introduction of CB. The incorporation of CB also exhibited the crosslink density of the rubber composites, as validated by swelling tests. We also observed the enhancement in tensile strength and other mechanical properties upon CB infiltration. The thermal stability of E9B1/CB30 was the highest. Overall, the study provided insights into the behavior of EPDM/PB/CB composites, suggesting their potential in a wide array of applications, especially where resilience, durability, and improved mechanical properties are important.

Acknowledgement

This work was supported by the Technology Innovation Program (or Industrial Strategic Technology Development Program-Material Components Technology Development Program) (No. 20011433, Extremely cold-resistant anti-vibration elastomer with EPDM) funded by the Ministry of Trade, Industry & Energy (MOTIE, Korea). This work was supported by the National Research Foundation of Korea (NRF) grant funded by the Korea government (MSIT) (No. 2021R1G1A1011525, Rapid low-temperature curing of thermoset resins via microwave). This work was supported by

the Technology Innovation Program (or Industrial Strategic Technology Development Program- Nano fusion innovative product technology development) (No. 20014475, Anti-fog nano-composite-based head lamp with <10% of low moisture adsorption in surface area) funded By the Ministry of Trade, Industry & Energy (MOTIE, Korea). This work was supported by the Technology Innovation Program (or Industrial Strategic Technology Development Program- Automobile industry technology development) (20015803, High performance composite-based battery pack case for electric vehicles via hybrid structure and weight lightening technology) funded By the Ministry of Trade, Industry & Energy (MOTIE, Korea). This work was supported by the Technology development Program (Antistatic extrudable carbon nanotube/polymer composites with 10^6-10^8 ohm/sq of surface resistance for display tray: S3111196) funded by the Ministry of SMEs and Startups (MSS, Korea). This research was supported by Research and Business Development Program through the Korea Institute for Advancement of Technology (KIAT) funded by the Ministry of Trade, Industry and Energy (MOTIE) (Development of one step black epoxy bonding film for micro LED display, grant number: P0018198). This work was supported by the Technological Innovation R&D Program (Development of metal-polymer heterojunction bonding technology using metal surface treatment and compatibilizing agents for lightweighting: S3236143) funded by the Ministry of SMEs and Startups (MSS, Korea). This work was supported by ITECH R&D program of MOTIE/KEIT [Project No. 20024384, Development of a battery housing cover using high orientation composite material with a fiber content of 40% and using recycled fibers and engineering plastics]. This research was also supported by Advanced Materials Analysis Center, The University of Suwon.

Conflict of Interest: The authors declare that there is no conflict of interest.

References

1. M. Molberg, Y. Leterrier, C. J. G. Plummer, C. Walder, C. Löwe, D. M. Opris, F. A. Nüesch, S. Bauer, and J.-A. E. Månson, "Frequency Dependent Dielectric and Mechanical Behavior of Elastomers for Actuator Applications", *J. Appl. Phys.*, **106**, 054112 (2009).
2. D. M. Opris, "Polar Elastomers as Novel Materials for Electromechanical Actuator Applications", *Adv. Mater.*, **30**, 1703678 (2018).
3. J.-H. Lee, S. Park, Y. S. Kim, D.-G. Kim, and S. Ahn, "Covalent Adaptable Liquid Crystal Elastomers Comprising Thiourea Bonds: Reprocessing, Reprogramming and Actuation", *Elast. Compos.*, **57**, 55 (2022).
4. U. Jung and S.-S. Choi, "Characteristics in Densities and Shapes of Various Particles Produced by Friction between Tire Tread and Road Surface", *Elast. Compos.*, **57**, 92 (2022).
5. S.-H. Lee, S.-Y. Park, K.-H. Chung, and K.-S. Jang, "Phlogopite-Reinforced Natural Rubber (NR)/Ethylene-Propylene-Diene Monomer Rubber (EPDM) Composites with Aminosilane Compatibilizer", *Polymers*, **13**, 2318 (2021).
6. S.-H. Lee, G.-W. Park, H.-J. Kim, K. Chung, and K.-S. Jang, "Effects of Filler Functionalization on Filler-Embedded Natural Rubber/Ethylene-Propylene-Diene Monomer Composites", *Polymers*, **14**, 3502 (2022).
7. A. E.-A. A. El-Wakil, S. El-Mogy, S. F. Halim, and A. Abdel-Hakim, "Enhancement of Aging Resistance of EPDM Rubber by Natural Rubber-g-N (4-Phenylenediamine) Maleimide as a Grafted Antioxidant", *J. Vinyl Addit. Technol.*, **28**, 367 (2022).
8. K.-R. Ha, J.-C. Lee, T.-G. Kim, and K.-S. Hwang, "Studies on the Ozone Resistance and Physical Properties of SBR/EPDM Blend Compound due to EPDM Content Variation", *Elast. Compos.*, **43**, 8 (2008).
9. Y. Shoda, D. Aoki, K. Tsunoda, and H. Otsuka, "Polybutadiene Rubbers with Urethane Linkages Prepared by a Dynamic Covalent Approach for Tire Applications", *Polymer*, **202**, 122700 (2020).
10. T. Tadaki, "Recent Advances in Polybutadienes", *Int. Polym. Sci. Technol.*, **31**, 5 (2004).
11. L. Dong, W. Zhou, X. Sui, Z. Wang, H. Cai, P. Wu, J. Zuo, and X. Liu, "A Carboxyl-Terminated Polybutadiene Liquid Rubber Modified Epoxy Resin with Enhanced Toughness and Excellent Electrical Properties", *J. Electron. Mater.*, **45**, 3776 (2016).
12. Y. Wang, Z. Yu, A. D. Phule, Y. Zhao, S. Wen, and Z. X. Zhang, "A Lightweight, Abrasion-Resistant Polybutadiene Rubber/Styrene Butadiene Rubber Foam Prepared by Three-Step Process for Footwear Outsole Applications", *Macromol. Mater. Eng.*, **307**, 2100702 (2022).
13. J.-H. Go and C.-S. Ha, "Rheology and Properties of EPDM/BR Blends with or without a Homogenizing Agent or a Coupling Agent", *J. Appl. Polym. Sci.*, **62**, 509 (1996).
14. A. Alipour, G. Naderi, G. R. Bakhshandeh, H. Vali, and S. Shokoohi, "Elastomer Nanocomposites Based on NR/EPDM/Organoclay: Morphology and Properties", *Int. Polym. Process*, **26**, 48 (2011).

15. H. Boukfessa, B. Bezzazi, H. Boukfessa, and B. Bezzazi, "The Effect of Carbon Black on the Curing and Mechanical Properties of Natural Rubber/Acrylonitrile-Butadiene Rubber Composites", *J. Appl. Res. Technol.*, **19**, 194 (2021).
16. A. Eldeeb, E. Taha, and M. Abd ElKader, "Investigation of an Insulating Waste Conscious Material For Sustainable Building Application", *Egypt. J. Chem*., **64**, 2305 (2021).
17. C. Darko, "The Link between Swelling Ratios and Physical Properties of EPDM Rubber Compound Having Different Oil Amounts", *J. Polym. Res*., **29**, 325 (2022).
18. M. van Duin and H. Dikland, "A Chemical Modification Approach for Improving the Oil Resistance of Ethylene–Propylene Copolymers", *Polym. Degrad. Stab*., **92**, 2287 (2007).
19. K. Adamska, A. Voelkel, and A. Berlińska, "The Solubility Parameter for Biomedical Polymers—Application of Inverse Gas Chromatography", *J. Pharm. Biomed. Anal.*, **127**, 202 (2016).
20. J. M. Kim, "Rheological Characteristics of the Theta-Shaped Polymer under Shear Flow", *Korea-Aust. Rheol. J*., **34**, 381 (2022).
21. J. Choi, J. Lim, S. Han, H. Kim, H. J. Choi, and Y. Seo, "How to Resolve the Trade-off between Performance and Long-Term Stability of Magnetorheological Fluids", *Korea-Aust. Rheol. J*., **34**, 243 (2022).
22. J. Seo, W. Kim, S. Bae, and J. Kim, "Influence of Loading Procedure of Liquid Butadiene Rubber on Properties of Silica-Filled Tire Tread Compounds", *Elast. Compos*., **57**, 129 (2022).